Heat Shield Mass Minimization for an Aerocapture Mission to Neptune

Antonio Mazzaracchio
Astronautical, Electrical, and Energetic Engineering Department,
Sapienza University of Rome, Rome, Italy
a_mazzaracchio@hotmail.com

[Received on 12/11/2013; Accepted on 19/12/2013]

Abstract
This paper discusses the sizing of the heat shield of a lifting-body spacecraft, protected by a rigid aeroshell, to minimize its mass for a future aerocapture mission to Neptune. Reducing the heat shield mass is a primary requirement for the mission design because the high expected heat loads can raise the value of its mass fraction to levels that would be unacceptable for the successful execution of the mission. The heat shield is divided into several regions, each of which is characterized by different levels of the entering heat flux. Its mass is minimized by identifying the most suitable materials to be used in the different zones and by determining their minimum thicknesses. To accomplish these tasks, a mapping is established a priori based on a common case treated in the literature. The analysis demonstrates that to minimize the mass for this vehicle, it is necessary to adopt a heat shield composed of different ablative materials that vary depending on the area to be protected. The front part of the spacecraft, near the stagnation point, should be protected exclusively by carbon phenolic, a high-density material, using substantial thicknesses, whereas thinner, lower-density ablative materials should be used to protect the ventral and dorsal regions. The frontal area alone constitutes approximately half of the entire mass of the heat shield while covering less than 10% the total surface.

1. INTRODUCTION

There is widespread interest in potential missions to Neptune; as in other cases of celestial bodies with atmospheres, options for exploring this planet include the use of both direct entry probes and missions with aerocapture of an orbiter [1]. However, the spacecraft must be equipped with an efficient thermal protection system (TPS) for protection and isolation from the effects of, in this case, very intense heating to which it will be subjected during its hypersonic flight across the planetary atmosphere. Incidentally, in an aerocapture mission, the aerodynamic drag encountered while crossing the planetary atmospheres is used in place of a conventional propulsion system to decelerate the vehicle until it reaches a stable orbit around the planet. As a result, the aerocapture permits considerable savings in the total mass of the vehicle compared to a solution with propulsive deceleration, in the case where both options are feasible. For direct entry probes to Neptune, an entry speed of approximately 28–32 km/s is expected, with very high entering heat fluxes. In particular, the entering heat fluxes will be greater than those for entering the Venus atmosphere but still lower than those for entering the Jupiter atmosphere. The leading candidate material for the front portion of the TPS is a high-density carbon phenolic with a composition that is most likely different from the materials used for the Pioneer Venus and Galileo missions. For this reason, this material will be characterized and qualified ex novo. With respect to the possibility of an aerocapture to Neptune, some feasibility analyses have demonstrated the need for a vehicle with a rigid aeroshell with a high aerodynamic efficiency ($L/D \approx 0.8$), undoubtedly greater than the one offered by a classic vehicle with a blunt conical profile. Entry speeds on the order of 30 km/s are expected, with a consequent total heat flux in the stagnation region— depending, inter alia, on the aerodynamic configuration of the vehicle—in the range of 10–15 kW/cm^2. These fluxes generate large thermal loads, in the range of 1,000–1,500 kJ/cm^2, due to the long duration of the atmospheric transit to accomplish the aerocapture maneuver. The concomitant presence of high fluxes and high thermal loads represent a complex technological challenge at the TPS level. These facts circumscribe the choice of the possible candidates to fully dense carbonaceous materials, even if the

required thickness exceeds the current constructive capacity to obtain a uniform, reliable composite. In the zones distant from the stagnation region, the thermal fluxes are lower but the resulting thermal loads still remain very high. For such zones, the adoptable solutions can be diversified with the use of, for example, medium-density ablative materials.

This paper considers the optimal sizing of the heat shield of a vehicle for a future aerocapture mission to Neptune, performed using a thermal analysis tool developed by the author and presented in Refs. 2, 3, and 4. The vehicle is considered to be protected by a rigid aeroshell provided with a heat shield divided into several regions characterized by different entering heat fluxes. The objectives of the analysis were to identify the most suitable materials to be used in the different areas of the heat shield and determine their minimum thicknesses, starting from a mapping established a priori based on the data available in the literature. The analysis approach is then applied to the optimization (minimization) of the mass of the TPS alone without regard to the total mass of the vehicle [3]. This case has only been addressed from the thermal perspective, starting from a trajectory and aero-thermal conditions that have been previously defined. Following this introduction, a review of the case study (the modeling assumptions and the vehicle, mission, and TPS materials considered) is presented in Section 2, and the relevant results and analyses are discussed in Section 3. Finally, Section 4 offers a summary and conclusions.

2. CASE STUDY

The goal of the case study is to minimize the mass of the TPS of a rigid aeroshell of a spacecraft to be used in a very demanding aerocapture mission to Neptune. The high expected heat loads can increase the value of the heat shield mass fraction to levels that would be unacceptable for the successful execution of the mission. In fact, the relevance of the masses involved, the existing propulsion problems, and the global energy issues for the fulfillment of the mission are such that the containment of the TPS mass forms the basis of the possibility of housing the payload, as explained in Subsection 2.3. The overall design is very complex and beyond the scope of this paper. The focus of the analysis described in this paper is the identification of the optimal composition of the TPS, i.e., the types of materials to be used and their thicknesses, for a type of vehicle widely studied in the literature concerning aerocapture to Neptune. The optimal configuration of the heat shield has been researched for a mission with the values of the expected entering heat fluxes assigned and the TPS mapping given. This mapping divides the TPS into various zones subjected to different values of heat flux. For this purpose, various materials available today for such extreme operating conditions were compared.

2.1 Assumptions

The study hypotheses assumed for this specific case are as follows:

- The thermal analysis is decoupled from the dynamic problem: the trajectory data and entering heat fluxes, depending on the location of the various areas in which the heat shield can be considered subdivided, are taken from a study by Laub and Chen [5].
- The TPS is configured from multiple materials, and each material is analyzed independently of the presence of the other materials.
- The maximum acceptable temperature for the bond-line, i.e., the adhesive junction layer between the heat shield and substructure, $T_{BL,lim}$, is fixed at 400 °C.
- The substructure is assumed to be constituted by a sandwich of thin sheets of carbon-carbon and aluminum honeycomb with a total thickness of 25.4 mm. The thermal characteristics and physical properties of the composite are derived from Ref. 6. The substructure is considered an integral part of the TPS even though the thermal characteristics of the adhesive layer are not considered in the thermal model used.

2.2 Vehicle

In the aerodynamic configuration of the vehicle, the primary objectives are as follows: to obtain a lift-to-drag ratio (L/D) of approximately 0.8, to minimize the ballistic coefficient (m/C_DS), to maximize the volumetric efficiency, and ultimately to produce a configuration that is compatible with the structure of the launch vehicle. The geometric shape considered is that of a “flattened ellipsled” body, i.e., constituted by an ellipsoidal front portion followed by a cylindrical part with an elliptical cross section whose final shape is obtained by crushing the lower minor semi-axis of the ellipse (Figure 1).

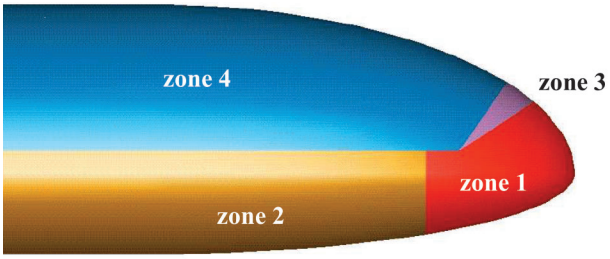

Figure 1. Flattened ellipsled vehicle for a Neptune aerocapture (side view).

Figure 1 also illustrates the subdivision of the external surface of the spacecraft in four different zones, for which it is possible to employ different materials and thicknesses, based on the thermal loads expected, to optimize the total mass of the heat shield. Zone 1 is the region near the stagnation point, zone 2 is the ventral area (forebody), zone 3 is the rear-nose area, and zone 4 is the dorsal area (afterbody).

Various theoretical investigations of two configurations of the flattened ellipsled vehicle—a "large" configuration with a length of 5.50 m and a "small" configuration with a length of 2.28 m, approximately half that of the former—are described in the literature. A ballistic coefficient of 400 kg/m^2 is expected for the "large" configuration, whereas the expected value for the "small" configuration is 895 kg/m^2, with an aerodynamic angle of attack of 40° in both cases. The "small" configuration type was chosen for the case study presented here.

2.3 Mission

A type of mission to Neptune hypothesized in the literature [5, 7, 8] assumes a launch in February 2017, for reasons related to the necessary use of an Earth–Jupiter or Venus–Jupiter gravity-assist maneuver (one or the other, depending on the type of propulsion planned), with a travel time of just over 10 years and an estimated entry speed into the Neptune atmosphere of approximately 28–30 km/s. The overall mission is designed to put a vehicle consisting of an orbiter and two identical probes into orbit around Neptune for scientific measurements on the planet and its main moon, Triton. The estimated total weight of the vehicle is approximately 2,000 kg. Figure 2 illustrates the aerocapture phase of the mission.

The level of the heat flux, with respect to the flight time in the atmosphere, expected at the stagnation point (zone 1 in Figure 1), is taken and tailored from Ref. 5 and is shown in Figure 3.

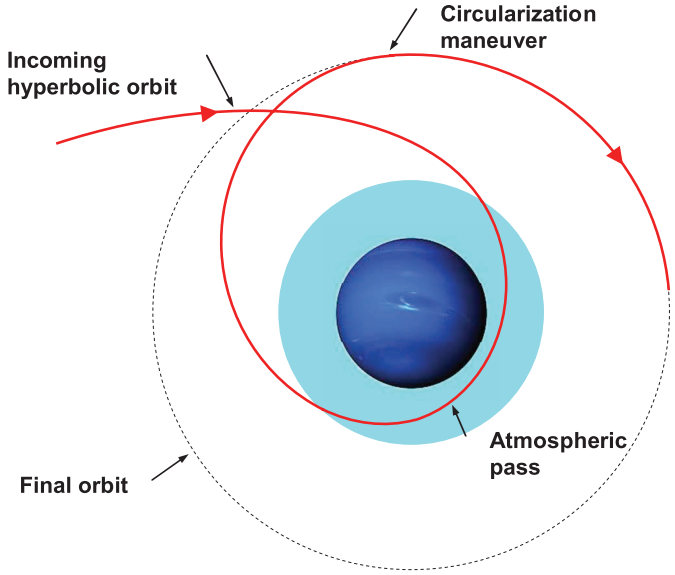

Figure 2. Schematic view of a Neptune aerocapture trajectory.

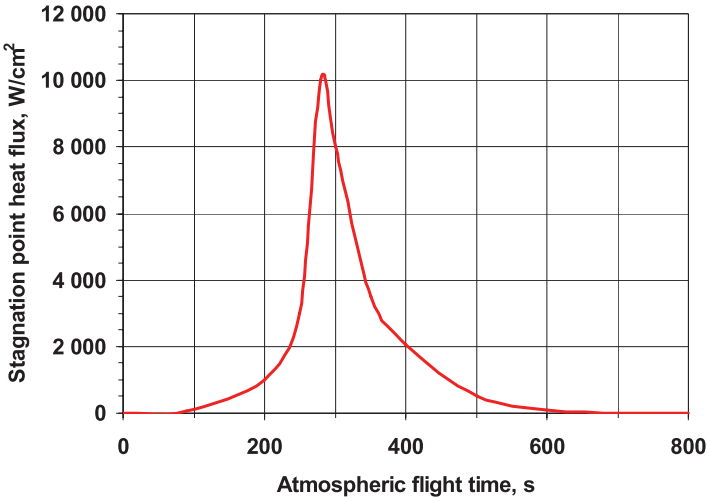

Figure 3. Neptune aerocapture: heat flux at the stagnation point.

For other areas of the spacecraft, the values of the entering heat flux were calculated according to the performance shown in Ref. 5, scaling the flux at the stagnation point by means of suitable reduction factors. Zones 3 and 4 are considered to be subject to the same level of heating.

2.4 TPS materials

There is a wide range of materials that can be used for thermal protection of spacecraft. A brief overview of the best-known ablative materials used to date by NASA is provided below. The details of their thermal and physical properties can be found in the cited references. Purely ceramic materials, such as silicone impregnated reusable ceramic ablator (SIRCA), are not analyzed here. One of the most popular materials used for ablative shields is carbon phenolic, which is very effective but has the disadvantage of a high density and thus a high thermal conductivity (the thermal conductivity of a material is proportional to its density). If the level of heat flux to which the vehicle is subjected during reentry is insufficient to trigger the pyrolysis, the high conductivity of the material may allow the heat flow to come into contact with the part to be protected. Consequently, carbon phenolic is not appropriate for reduced heat fluxes. In such cases, it is preferable to use lower-density materials. The ablative materials considered here are the following: PICA-15, SLA-561V, 5026-H AVCOAT CG, and FM 5055 CP, the latter of which are available in two versions, "standard density" (fully dense, FD) and "low density" (reduced density, RD). Table 1 summarizes the reference values of the main physical and thermal properties of the various materials. In reality, the properties of the materials are functions of temperature and pressure; this dependence has been taken into account in the study.

Table 1. Main characteristics of ablative TPS materials.

		Density, kg/m^3	Specific heat, J/(kg K)	Thermal conductivity, W/(m K)
PICA-15	Virgin	240	1,715	0.30
	Char	96	4,605	1.17–1.71
SLA-561V	Virgin	232	1,260	0.04
	Char	128	1,670	0.10–0.33
AVCOAT 5026-HCG	Virgin	512	1,550	0.19
	Char	256	1,925	0.28–1.38
FM 5055 FDCP	Virgin	1,460	1,060	1.02
	Char	1,275	2,460	1.24
FM 5055 RDCP	Virgin	1,037	1,500	1.32
	Char	519	2,100	2.75–14.28

2.4.1 PICA-15

Phenolic impregnated carbon ablator (PICA) is mainly known in its PICA-15 form. PICA-15, hereinafter also referred to simply as PICA, to date has been used in the Stardust and Mars Science Laboratory probes. PICA was developed relatively recently by NASA's Ames Research Center. It is characterized by extremely low density and thermal conductivity compared to other ablative materials, particularly with respect to the classic carbon phenolic, but has nonetheless excellent ablative characteristics for high heat fluxes. PICA, which is formed by impregnating an insulating matrix of chopped carbon fibers with a commercial thermosetting resin phenol–formaldehyde (SC 1008), has a final density of 0.22–0.32 g/cm^3 and is characterized by the following mass composition: 92% carbon, 4.9% oxygen, 2.2% hydrogen, and 0.9% nitrogen. Its ablation rate increases with the entering heat flux, and the predominant chemical species in the char are carbon (C) and carbon monoxide (CO) [9]. The high porosity of the resulting composite is the reason for the low density and conductivity values. The properties of PICA were derived from Refs. 10, 11, and 12.

2.4.2 SLA-561V

Super-lightweight ablator (SLA), called SLA-561V, is the material chosen by NASA for all Mars missions undertaken to date. SLA-561V is manufactured by Lockheed Martin and consists of phenolic and ceramic micro-balloons, fiberglass, cork, and elastomeric silicone in a phenolic honeycomb. The properties of SLA-561V, hereinafter also referred to simply as SLA, are taken from Refs. 10, 11, and 14.

2.4.3 AVCOAT 5026 HCG

AVCOAT 5026-HCG is an ablative material consisting of a phenolic resin called a novolac and a fiberglass honeycomb. The realization process provides for the direct bonding of the honeycomb to the substructure, with subsequent filling of each individual cell with the resin. NASA used this material for the command modules of the Apollo program and recently proposed its use, based on a new formulation developed as a result of current environmental regulations, for the next generation of the Orion vehicles. The char of the material is mainly composed of silicon and carbon; only carbon generates exothermic reactions of oxidation, whereas silicon may be considered an inert material. The characteristics and properties of AVCOAT 5026-HCG, hereinafter also referred to as AVCOAT, are taken from Ref. 10.

2.4.4 FM 5055 CP

Fully dense carbon phenolic (FDCP), developed in the 1960s, is the only material that has demonstrated operational capacity and reliable performance for heat fluxes in the range of 1–5 kW/cm^2 at pressures of 1–5 atm. Thus, FDCP is the only flight-qualified material in severe aerothermal environments. The version of carbon phenolic called FM 5055 was used in the Pioneer Venus and Galileo missions. Carbon phenolic composites are made with carbon fibers impregnated with phenolic resins polymerized in an autoclave or under heated hydraulic presses. The final product obtained has a very high density compared to the other available ablative materials. In contrast, reduced density carbon phenolic (RDCP) is a "theoretical" material based on the perspective of maintaining a good level of ablative performance typical of carbon phenolic composites while simultaneously improving the thermal insulation characteristics through a reduction in density. These materials were briefly studied in 1980, with the execution of a few encouraging tests. All thermophysical properties of carbon phenolic are taken from Ref. 10.

3. RESULTS AND ANALYSIS

3.1 TPS sizing

All ablative materials presented in Section 2.4 were tested for each of the four zones of expected entering heat flux into which the TPS is assumed to be subdivided (see Figure 1). Tables 2, 3, and 4 present the main characteristic parameters obtained using each material in each TPS zone. The absence of data for a certain material and zone means a feasible solution was not obtained for the use of that material in that zone. Consequently, the material cannot be regarded as a candidate for use in that particular zone of the heat shield. In the last row of each table, the value of the "areal density", i.e., the product of the density of the material and the required initial thickness, is provided.

Table 2. Heat shield characteristic parameters: frontal area (zone 1).

	SLA	PICA	AVCOAT	RDCP	FDCP
Density, kg/m^3	**232**	**240**	**512**	**1,037**	**1,460**
Initial thickness of the ablative layer, cm	-	-	-	-	14.56
Final thickness of the ablative layer, cm	-	-	-	-	2.69
Surface recession, cm	-	-	-	-	11.87
Maximum surface temperature, K	-	-	-	-	47,48
Total heat load, J/cm^2	-	-	-	-	1,124,996
Areal density, g/cm^2	-	-	-	-	21.26

Table 3. Heat shield characteristic parameters: forebody (zone 2).

	SLA	PICA	AVCOAT	RDCP	FDCP
Density, kg/m^3	**232**	**240**	**512**	**1,037**	**1,460**
Initial thickness of the ablative layer, cm	-	-	9.98	9.92	5.65
Final thickness of the ablative layer, cm	-	-	3.41	7.24	2.97
Surface recession, cm	-	-	6.57	2.68	2.68
Maximum surface temperature, K	-	-	3,896	3,573	3,338
Total heat load, J/cm^2	-	-	314,999	314,999	314,999
Areal density, g/cm^2	-	-	5.11	10.29	8.25

Table 4. Heat shield characteristic parameters: afterbody (zones 3 and 4).

	SLA	PICA	AVCOAT	RDCP	FDCP
Density, kg/m^3	**232**	**240**	**512**	**1,037**	**1,460**
Initial thickness of the ablative layer, cm	2.88	5.19	3.77	4.51	2.75
Final thickness of the ablative layer, cm	1.69	5.08	3.65	4.51	2.75
Surface recession, cm	1.19	0.11	0.12	0.00	0.00
Maximum surface temperature, K	2,064	2,410	2,388	2,079	2,330
Total heat load, J/cm^2	31,500	31,500	31,500	31,500	31,500
Areal density, g/cm^2	0.67	1.25	1.93	4.67	4.01

The areal density can be adopted as a criterion for selection of the material when it is necessary to minimize the mass of the TPS, as in this case. For zone 1, FDCP is the only usable material despite its substantial initial thickness (14.56 cm). At the end of the mission, the surface recession is equal to 11.87 cm. The high maximum surface temperature observed, approximately 4,700 K, is still compatible with the capability of the material [15]. Finally, for high thermal fluxes, such as those provided for the area around the stagnation point, the materials with the lowest density cannot be employed. For zone 2, the ventral part of the vehicle, it is possible to employ AVCOAT and both types of carbon phenolic. AVCOAT is the material characterized by the lower areal density in this case, although it has the greater initial thickness, equal to approximately 10 cm. Its surface recession, equal to 6.6 cm, is considerable. All five materials tested are suitable for zones 3 and 4, the top rear-nose and dorsal part of the vehicle, respectively. Zone 4 is the zone with the largest area, covering more than half of the vehicle; thus, the choice of a material with low areal density is critical in this case. SLA-561V appears to be the most efficient material for this purpose because it has the smallest initial thickness and lowest density of the materials considered. In this area, neither RDCP nor FDCP are subjected to surface recession. Finally, the thermal load in zone 1 is 3.6 times greater than that in zone 2 and approximately 36 times greater than those in zones 3 and 4. Figures 4, 5, and 6 provide a visual comparison among the materials that can be employed for each TPS zone, illustrating the values of the areal density, initial thickness, and expected surface recession, respectively. FDCP is more efficient than RDCP for the aerocapture case under consideration.

Based on considerations discussed, the feasible combination that leads to the heat shield with the smallest mass is shown in Fig 7.

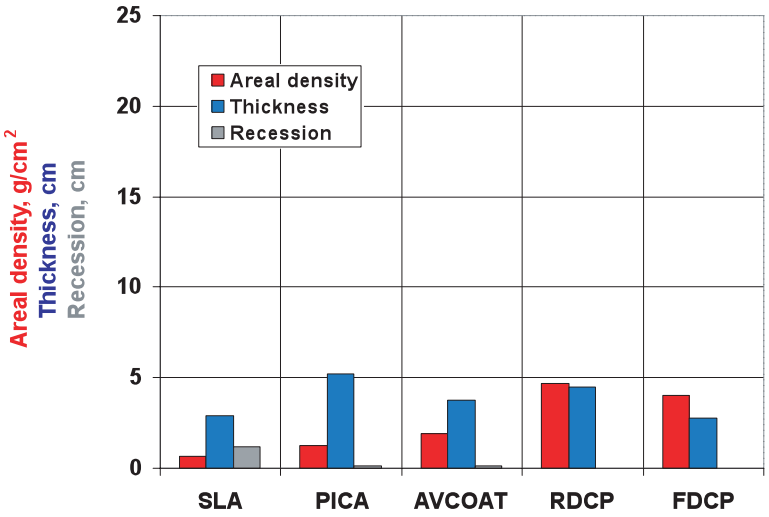

Figure 4. TPS sizing: frontal area (zone 1).

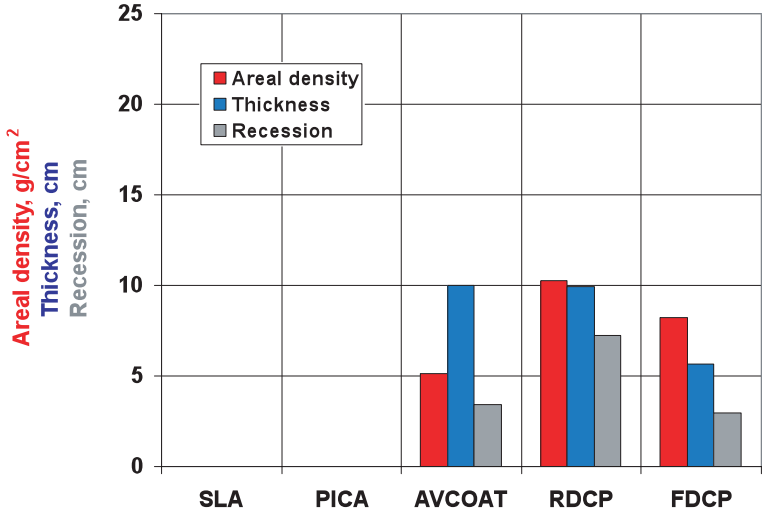

Figure 5. TPS sizing: forebody (zone 2).

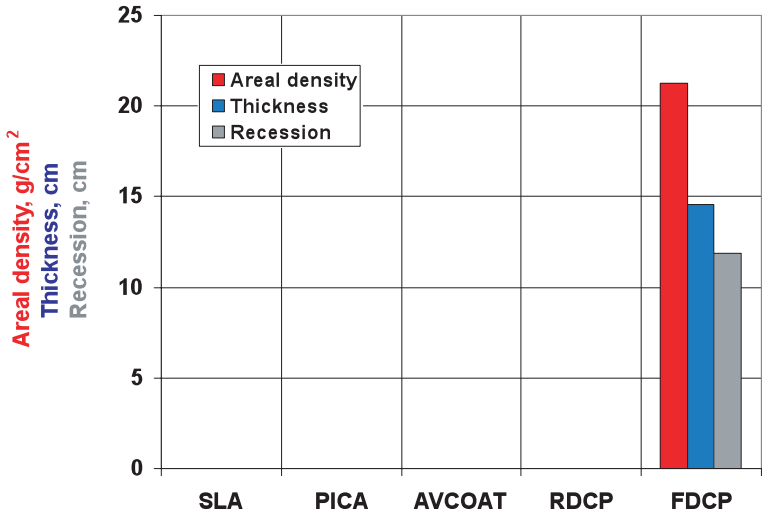

Figure 6. TPS sizing: afterbody (zones 3 and 4).

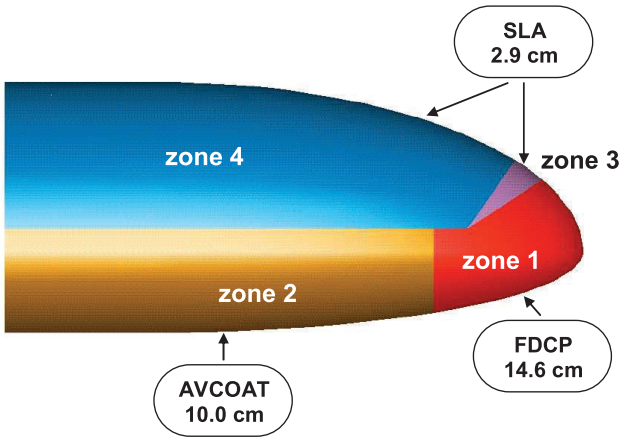

Figure 7. Neptune aerocapture: TPS optimal configuration (materials and thickness).

Figures 8 and 9 compare the resulting percentage fractions for the surface and mass of each TPS zone, respectively. The main observations are as follows:

- The coverage of zone 1, which occupies approximately 10% of the total surface, accounts for almost half of the total mass of the TPS.
- More than half of the vehicle (zone 4) can be protected with a mass of less than 8% of the total mass of the entire heat shield.
- The total mass of the resulting heat shield is 483.15 kg. Its mass fraction, with respect to the total mass of the vehicle, is equal to approximately 24%, which represents a very interesting value for this type of mission.

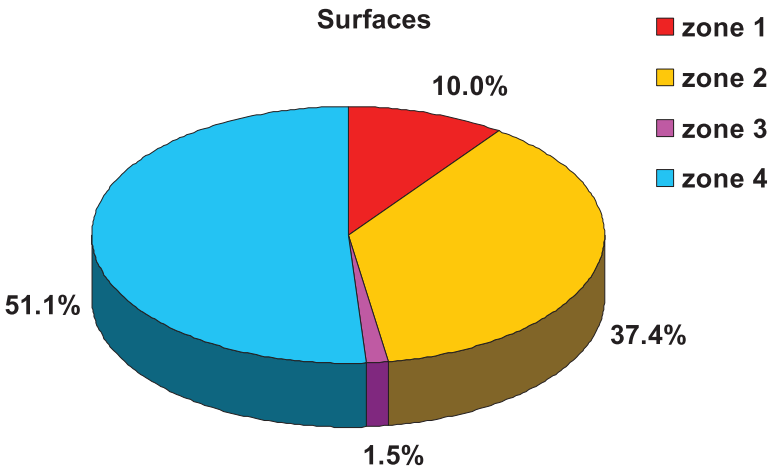

Figure 8. Aerocapture to Neptune: TPS surface percentage fractions.

3.2 The thermal field

The evolution of the temperature and the state of the various layers that originate within the ablative materials were also analyzed. Figure 10 illustrates the case study detailed in nine successive instants, at intervals of 100 s, and at the end of flight. The images illustrate the situation in the four different zones of the TPS and represent the trends in the temperature with depth in each material, as well as the state of the materials and the thicknesses of the various layers of the heat shield as a function of flight time. The various images illustrate how the materials react effectively to heating over time, illustrating their thermal protection capabilities. The slopes of the temperature curves versus thickness are

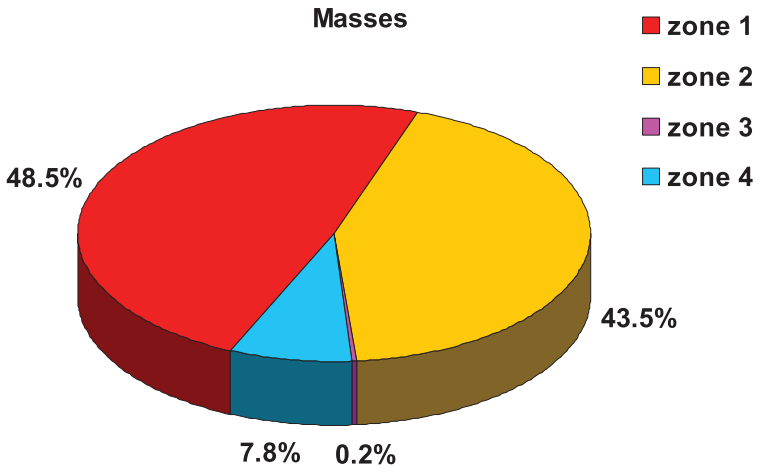

Figure 9. Neptune aerocapture: TPS mass percentage fractions.

remarkable in the reaction zones and in the mature char, while the slopes in the virgin material layers indicate that here, these materials do not undergo appreciable temperature variations. Near the end of the flight, all of the virgin material in all zones has undergone the process of pyrolysis and is no longer present, while the process of surface cooling surface has started (as detectable by the formation of a ripple in the temperature curve). The consumption of the entire ablative virgin layer is one of the results of the theoretical optimization process—the search for the minimum thickness—which does not support the assumption that a thickness factor of safety should be adopted in this case.

4. SUMMARY AND CONCLUSIONS

A heat shield optimization problem for a rigid aeroshell for an aerocapture mission to Neptune is presented in this paper. The mission studied represents a very severe test bed for the design of a TPS able to cope with the extremely high heat fluxes peaks and total thermal loads expected. The considerable values of the thermal loads are due to the long duration of the aerocapture trajectories and require very substantial thicknesses for the TPS. High thicknesses can create problems in the implementation and product manufacturing phases and can generate doubts about the convenience of the mission due to the significant heat shield mass required. A mission profile based on a common case treated in the literature was used in the analysis described in this paper, from which the atmospheric phase trajectory and related thermal flows expected were derived. The results demonstrate that for this case, to minimize the TPS mass, it is necessary to use a shield with multiple ablative materials based on the area to be protected. The frontal zone may be protected only by very dense materials, such as carbon phenolic of a significant thickness, whereas the ventral and dorsal regions can be protected using thinner, lower-density ablative materials, with a consequent reduction in the total mass of the TPS. The frontal area alone constitutes approximately half of the entire mass of the shield while covering less than 10% of the total surface. The analysis of the thermal field that is established in the heat shield demonstrates the high efficiency of the heat shield in providing thermal insulation for the substructure.

ACKNOWLEDGEMENTS

The authors would like to thank Salvatore Cimmino for providing the tool for the graphical analysis of the thermal field.

Figure 10. Neptune aerocapture: temperature vs. depth in the material, state of the material, and thickness of the various layers of the heat shield as a function of the time of flight.

NOMENCLATURE

C_D = Drag coefficient
D = Drag, N
L = Lift, N
m = Mass, kg
S = Vehicle reference surface, m^2
$T_{BL,lim}$ = Bond-line limit temperature, K

REFERENCES

[1] Laub, B., and Venkatapathy, E., Thermal Protection System Technology and Facility Needs for Demanding Future Planetary Missions, *International Workshop on Planetary Probe Atmospheric Entry and Descent Trajectory Analysis and Science, Lisbon*, Portugal, 6-9 October 2003.

[2] Mazzaracchio, A., and Marchetti, M., A Probabilistic Sizing Tool and Monte Carlo Analysis for Entry Vehicle Ablative Thermal Protection Systems, *Acta Astronautica*, 2010, 66 (5-6), 821-835. DOI: 10.1016/j.actaastro.2009.08.033

[3] Mazzaracchio, A., Thermal Protection System and Trajectory Optimization for Orbital Plane Change Aeroassisted Maneuver, *Journal of Aerospace Technology and Management*, 2013, 5 (1), 49-64. DOI: 10.5028/jatm.v5i1.208.

[4] Mazzaracchio, A., and Marchetti, M., Effect of Spacecraft Aerodynamics and Heat Shield Characteristics on Optimal Aeroassisted Transfer, *Engineering*, 2012, 4 (6), 307-320. DOI: 10.4236/eng.2012.46040.

[5] Laub, B., and Chen, Y-K., TPS Challenges for Neptune Aerocapture, *AIAA Paper 2004-5178*.

[6] Liechty, D. S., Aeroheating Analysis for the Mars Reconnaissance Orbiter with Comparison to Flight Data, *AIAA Paper 2006-3890*.

[7] Masciarelli, J. P., Westhelle, C. H., and Graves, C. A., Aerocapture Guidance Performance for the Neptune Orbiter, *AIAA Paper 2004-4954*.

[8] Lockwood, M. K., Neptune Aerocapture Systems Analysis, *AIAA Paper 2004-4951*.

[9] Olynick, D., Chen, Y.-K., and Tauber, M. E., Forebody TPS Sizing with Radiation and Ablation for the Stardust Sample Return Capsule, *AIAA 32nd Thermophysics Conference*, Atlanta, GA, June 23-25, 1997, AIAA Paper 1997-2474.

[10] Williams, S. D., and Curry, D. M., Thermal Protection Materials - Thermophysical Property Data, NASA RP 1289, 1992.

[11] Covington, M. A., Heinemann, J. M., Goldstein, H. E., Chen, Y.-K., Terrazas-Salinas, I., Balboni, J. A., Olejniczak, J., and Martinez, E. R., Performance of a Low Density Ablative Heat Shield Material, *37th AIAA Thermophysics Conference*, Paper No. AIAA-2004-2273, June 28-July 1, 2004, Portland, Oregon.

[12] Tran, H. K., Johnson, C. E., Rasky, D. J., Hui, F. C. L., Hsu, M.-T., Chen, T., Chen, Y.-K., Paragas, D., and Kobayashi, L., *Phenolic Impregnated Carbon Ablators (PICA) as Thermal Protection Systems for Discovery Missions*, NASA TM-110440, April 1997.

[13] Tran, H., Tauber, M., Henline, W., Tran, D., Cartledge, A., Hui, F., and Zimmerman, N., *Ames Research Center Shear Tests of SLA-561V Heat Shield Material for Mars-Pathfinder*, NASA TM-110402, September 1996.

[14] Seiferth, R. W., *Ablative Heat Shield Design for Space Shuttle*, NASA CR-132282, 1973.

[15] *Study of the Adaptability of Existing Hardware Designs to a Pioneer Saturn/Uranus Probe - Final Report*, Martin Marietta Corp., NASA-CR-137650, 1973.